THE JOURNAL OF BIOLOGICAL CHEMISTRY VOL. 291, NO. 34, pp. 17510–17522, August 19, 2016

The Molecular Chaperone Hsc70 Interacts with Tyrosine Hydroxylase to Regulate Enzyme Activity and Synaptic Vesicle Localization*

Received for publication, March 22, 2016, and in revised form, June 29, 2016 Published, JBC Papers in Press, June 30, 2016, DOI 10.1074/jbc.M116.728782

Leonardo A. Parra[‡], Tracy B. Baust[‡], Amanda D. Smith[§], Juliann D. Jaumotte[§], Michael J. Zigmond[§], Soledad Torres[¶], Rehana K. Leak[‖], Jose A. Pino[**], and Gonzalo E. Torres[1]**

*From the Departments of [‡]Neurobiology and [§]Neurology, University of Pittsburgh School of Medicine, Pittsburgh, Pennsylvania 15261, the [¶]Centro de Investigación y Modelamiento de Fenómenos Aleatorios Valparaíso, Faculty of Engineering, Universidad de Valparaíso, 2362905 Valparaíso, Chile, the [‖]Division of Pharmaceutical Sciences, Duquesne University, Pittsburgh, Pennsylvania 15282, and the **Department of Pharmacology and Therapeutics, University of Florida College of Medicine, Gainesville, Florida 32610*

We previously reported that the vesicular monoamine transporter 2 (VMAT2) is physically and functionally coupled with Hsc70 as well as with the dopamine synthesis enzymes tyrosine hydroxylase (TH) and aromatic amino acid decarboxylase, providing a novel mechanism for dopamine homeostasis regulation. Here we expand those findings to demonstrate that Hsc70 physically and functionally interacts with TH to regulate the enzyme activity and synaptic vesicle targeting. Co-immunoprecipitation assays performed in brain tissue and heterologous cells demonstrated that Hsc70 interacts with TH and aromatic amino acid decarboxylase. Furthermore, *in vitro* binding assays showed that TH directly binds the substrate binding and carboxyl-terminal domains of Hsc70. Immunocytochemical studies indicated that Hsc70 and TH co-localize in midbrain dopaminergic neurons. The functional significance of the Hsc70-TH interaction was then investigated using TH activity assays. In both dopaminergic MN9D cells and mouse brain synaptic vesicles, purified Hsc70 facilitated an increase in TH activity. Neither the closely related protein Hsp70 nor the unrelated Hsp60 altered TH activity, confirming the specificity of the Hsc70 effect. Overexpression of Hsc70 in dopaminergic MN9D cells consistently resulted in increased TH activity whereas knockdown of Hsc70 by short hairpin RNA resulted in decreased TH activity and dopamine levels. Finally, in cells with reduced levels of Hsc70, the amount of TH associated with synaptic vesicles was decreased. This effect was rescued by addition of purified Hsc70. Together, these data demonstrate a novel interaction between Hsc70 and TH that regulates the activity and localization of the enzyme to synaptic vesicles, suggesting an important role for Hsc70 in dopamine homeostasis.

Dopaminergic neurons within the substantia nigra and ventral tegmental area are the primary sources of the catecholamine neurotransmitter dopamine (DA).[2] Despite the fact that dopaminergic neurons account for less than 0.01% of all neurons, they play a significant role in brain function (1–3). Consequently, DA homeostasis is crucial for the preservation and regulation of physiological functions such as locomotion, cognition, neuroendocrine secretion, and motivated behaviors (4). Thus, it is not surprising that disruptions in the DA system have been implicated in several neurological and psychiatric disorders, including Parkinson disease, depression, schizophrenia, attention deficit hyperactivity disorder, Tourette syndrome, and drug addiction (4–8).

The DA life cycle consists of a series of highly regulated molecular events that are ultimately responsible for controlling DA homeostasis. Synthesis of DA occurs in the presynaptic terminals via two enzymatic reactions. First, tyrosine is converted into L-3,4-dihydroxyphenylalanine through the actions of the rate-limiting enzyme tyrosine hydroxylase (TH) (9, 10). Subsequently, aromatic amino acid decarboxylase (AADC) converts L-DOPA into DA (11). When synthesized, DA is packaged and stored within synaptic vesicles through the action of the vesicular monoamine transporter 2 (VMAT2) prior to undergoing regulated exocytosis through a complex series of protein interactions (12). DA, released from presynaptic neurons, then binds to pre- and postsynaptic DA receptors that mediate the actions of the neurotransmitter. A key step in determining the intensity and duration of DA signaling at synapses is reuptake of the transmitter back into nerve terminals by the plasma membrane DA transporter. Re-uptake through the DA transporter is the primary mechanism for the regulation of extracellular DA concentrations and, thus, the most effective way of terminating DA actions (13). The cleared DA is then repackaged into synaptic vesicles or is catabolized by monoamine oxidase (14). Although much research has focused on characterizing the life cycle of DA, many of the molecular details about DA homeostasis regulation remain unclear.

* This work was supported by National Institutes of Health Grant DA038598 (to G. E. T.). The authors declare that they have no conflicts of interest with the contents of this article. The content is solely the responsibility of the authors and does not necessarily represent the official views of the National Institutes of Health.

[1] To whom correspondence should be addressed: Dept. of Pharmacology and Therapeutics, University of Florida College of Medicine, 1200 Newell Dr., ARB R5-252, P. O. Box 100267, Gainesville, FL 32610-0267. Tel.: 352-273-8315; Fax: 352-392-3558; E-mail: gonzalotorres@ufl.edu.

[2] The abbreviations used are: DA, dopamine; TH, tyrosine hydroxylase; AADC, aromatic amino acid decarboxylase; SYPH, synaptophysin; GS, glutamine synthetase; SBD, substrate-binding domain; CTD, carboxyl-terminal domain; SV, synaptic vesicle; PNS, postnuclear supernatant; β-ME, β-mercaptoethanol; IB, immunoblot.

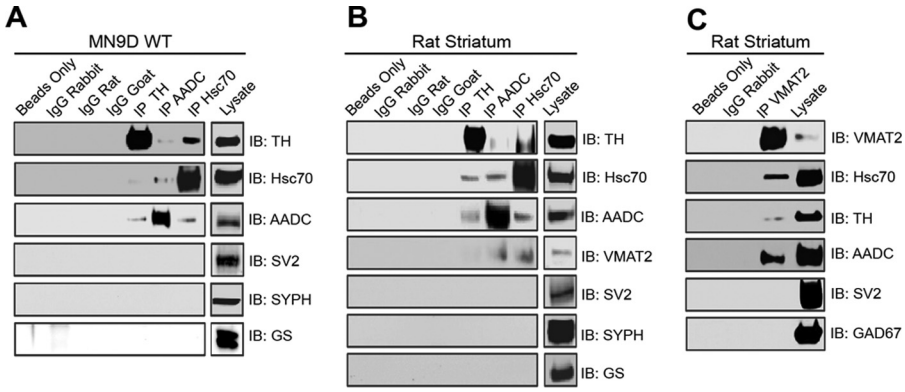

FIGURE 1. **HSC70, TH, AADC, and VMAT2 co-precipitate in MN9D cells and rat striatum.** *A* and *B*, co-immunoprecipitation (*IP*) experiments were performed by incubating MN9D cells (*A*) or rat striatum (*B*) lysates with anti-TH, anti-AADC, or anti-Hsc70 antibodies. SDS-PAGE and immunoblot (IB) analysis using the designated antibodies demonstrated co-precipitation of TH, AADC, and Hsc70. VMAT2 also co-precipitated with these proteins in rat striatum experiments. Unrelated vesicular and cytosolic proteins (SV2, SYPH, GS, and Hsp70) failed to co-immunoprecipitate. *C*, similar co-immunoprecipitation experiments were performed by incubating rat striatum with the VMAT2 antibody. SDS-PAGE and IB analysis using antibodies against VMAT2, Hsc70, TH, and AADC demonstrated that these proteins co-precipitate. IB analysis with antibodies against SV2 and GAD67 showed no co-precipitation. No bands were present in any of the immunoprecipitations performed using the nonspecific IgGs or beads only.

Recently, several protein-protein interactions implicated in DA homeostasis regulation have been identified (15). Indeed, we reported two such interactions involving DA synthesis and vesicular storage. First, we demonstrated that VMAT2 is functionally regulated by a physical interaction with the molecular chaperone heat shock cognate 70 (Hsc70) (16). Classically, Hsc70 has been known as a constitutively expressed protein responsible for mediating cellular processes such as folding, assembly, disassembly, and translocation of proteins (17). Our report describing the VMAT2-Hsc70 interaction was the first to suggest that Hsc70 may also have a regulatory role in monoamine storage. In a subsequent study, we reported that VMAT2 is also coupled to the enzymes that synthesize DA, TH, and AADC (18). Our data showed that TH and AADC were associated with synaptic vesicles and that DA synthesis through these enzymes was physically and functionally coupled to VMAT2-mediated transport into synaptic vesicles. However, the mechanism by which the enzymes responsible for DA synthesis are targeted to synaptic vesicles still remains elusive. In this study, we provide evidence that the molecular chaperone Hsc70 interacts with TH, regulates its activity, and promotes the targeting of the enzyme to synaptic vesicles.

Results

Hsc70 and TH Co-immunoprecipitate and Participate in a Biochemical Complex Involving VMAT2 and AADC—To examine whether Hsc70 has a role in DA synthesis, we first performed immunoprecipitation experiments investigating whether a physical interaction between Hsc70 and the enzymes responsible for DA synthesis, TH and AADC, exists. Lysates from the dopaminergic cell line MN9D were incubated with antibodies against Hsc70, TH, or AADC. Under each of these conditions, immunoblot analysis of these samples showed that Hsc70, TH, and AADC co-precipitated (Fig. 1*A*). As a negative control, MN9D lysates were also incubated with nonspecific IgGs or no antibody (beads only). No bands were present in any of these control samples when analyzed by immunoblot using the Hsc70, TH, or AADC antibodies. In the same manner, we repeated these immunoprecipitation experiments using rat striatum lysate. Again, immunoblot analysis demonstrated that Hsc70, TH, and AADC co-precipitated (Fig. 1*B*). No bands were present in any of the striatum samples incubated with either the nonspecific IgGs or beads only. In both MN9D and striatum lysate, immunoprecipitation with Hsc70, TH, or ADDC antibodies failed to co-precipitate the synaptic vesicle proteins SV2 or synaptophysin (SYPH) or the unrelated enzyme glutamine synthetase (GS) (Fig. 1, *A* and *B*), further demonstrating the specificity of the Hsc70-TH-AADC interaction.

We also analyzed the striatum immunoprecipitation experiments by immunoblot with the VMAT2 antibody. VMAT2 co-precipitates from striatum lysate incubated with the Hsc70 as well as TH and AADC antibodies. Importantly, all four proteins co-precipitated within the same experimental sample (Fig. 1*B*). In a final set of immunoprecipitation experiments, striatum lysate was incubated with a VMAT2 antibody. Again, immunoblot analysis of this sample showed that Hsc70, TH, AADC, and VMAT2 all co-precipitated (Fig. 1*C*). No bands were present in the samples incubated with the nonspecific IgG or beads alone. SV2 and glutamate decarboxylase 67 (GAD67) failed to co-precipitate with VMAT2, demonstrating the specificity of our results.

Next we examined the specificity of the TH-Hsc70 interaction by asking whether additional chaperones are able to co-immunoprecipitate with TH. Because the expression of the closely related Hsp70 is almost undetectable in MN9D cells, we induced its expression by heat shock. As shown in Fig. 2*A*, heat shock at 42 °C for 5 h induced a robust expression of Hsp70 in MN9D cells. However, under these conditions, immunoprecipitation of TH did not result in the co-precipitation of Hsp70. Similarly, we failed to detect an interaction between TH and the more distantly related chaperones Grp78 or Hsp90 (Fig. 2*B*), suggesting high specificity in the TH-Hsc70 interaction. Taken together, these experiments provided not only the first line of evidence showing that Hsc70 and TH physically interact in a specific manner but also suggests that Hsc70, TH, AADC, and

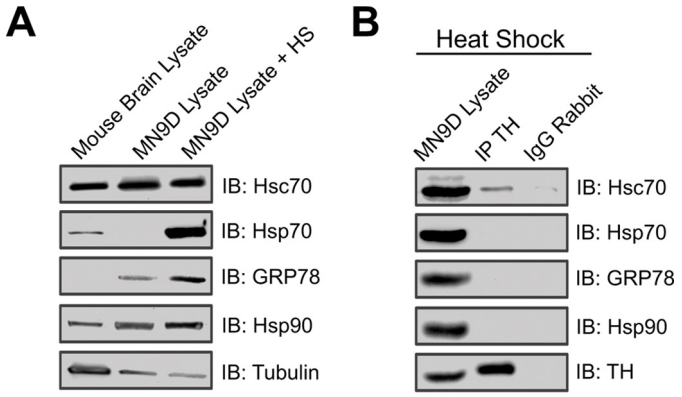

FIGURE 2. **Specificity of the interaction between TH and HSC70.** *A*, immunoblot analysis showing the expression of Hsc70, HSP70, GRP78, and HDP90 from MN9D cells under control conditions or after heat shock (*HS*). *B*, co-immunoprecipitation (*IP*) experiments were performed by incubating MN9D cell lysates with anti-TH antibody. SDS-PAGE and IB analysis using the designated antibodies demonstrated co-precipitation of Hsc70 but not HSP70, GRP78, or Hsp90. No bands were present in any of the immunoprecipitations performed using nonspecific IgGs.

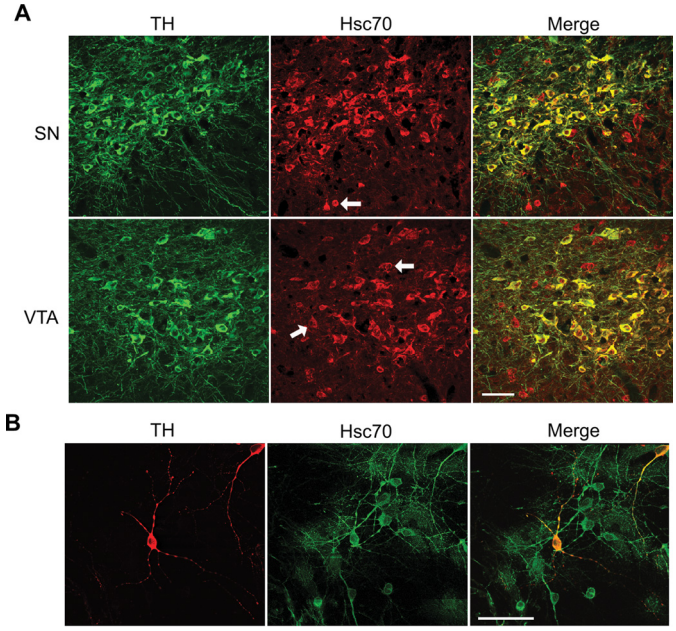

FIGURE 3. **Hsc70 and TH co-localize in brain dopamine neurons.** *A*, mouse midbrain sections of the substantia nigra (*SN*) and ventral tegmental area (*VTA*) were immunostained with polyclonal anti-TH (*green*, labeled with Alexa Fluor 488) and monoclonal Hsc70 (*red*, labeled with Alexa Fluor 555) antibodies. *B*, primary cell cultures from rat midbrain were immunostained with a polyclonal anti-TH (*red*, labeled with Alexa Fluor 555) and monoclonal Hsc70 antibodies (*green*, labeled with Alexa Fluor 488) antibodies. In both samples, merged images show that a majority of the TH-positive cells were dual-labeled with Hsc70 in both preparations (*A* and *B*, *right panels*). Only a few TH cells did not contain Hsc70. The co-localization of TH and Hsc70 extended into the process of the dopaminergic neurons. (*B*, *right panels*). *Scale bars* = 50 μm.

VMAT2 participate in a larger biochemical complex that links DA synthesis and vesicular storage.

Hsc70 and TH Co-localize in Midbrain Dopamine Neurons—To examine the biologic plausibility of the Hsc70/TH interaction, we next examined whether these two proteins are co-expressed and co-localized within dopaminergic neurons from mouse midbrain. Confocal microscopy revealed extensive TH (Fig. 3*A*, *left panels*) and Hsc70 (Fig. 3*A*, *center panels*) staining throughout both the substantia nigra (Fig. 3*A*, *top panels*) and ventral tegmental area (Fig. 3*A*, *bottom panels*). Merged images showed that a majority of the midbrain neurons in both the substantia nigra and ventral tegmental area were double-labeled with TH and Hsc70 antibodies (Fig. 3*A*, *right panels*). Only a few TH-positive cells did not contain Hsc70. This pattern would be expected based on the abundant nature of Hsc70 and support the hypothesis that TH and Hsc70 are both expressed in ventral midbrain dopaminergic neurons. We performed similar immunocytochemical studies from midbrain neuronal cultures. As expected, dopaminergic neurons comprised only a small fraction of the entire culture, as evidenced by the low density of TH+ cells (Fig. 3*B*, *left panel*). In contrast, the majority of the cultured cells exhibited robust Hsc70 staining (Fig. 3*B*, *center panel*). Nevertheless, extensive co-localization of TH and Hsc70 was exhibited within most of the dopaminergic neurons. Double staining with TH and Hsc70 antibodies revealed extensive overlap of TH and Hsc70 immunostaining along the neural processes in a clustering distribution pattern (Fig. 3*B*). These data provide further support of a presynaptic interaction between TH and Hsc70.

The Substrate-binding and Carboxyl-terminal Domains of Hsc70 Can Directly Interact with TH—Having demonstrated that Hsc70, TH, and AADC co-localize and co-immunoprecipitate, we next performed GST pulldown assays to delineate the domains of Hsc70 involved in the interaction with TH. Hsc70 contains different functional domains, including the ATPase domain (residues 1–373), substrate-binding domain (SBD, residues 373–540), and carboxyl-terminal domain (CTD, residues 540–650) (Fig. 4*A*). Lysates from MN9D cells were incubated with GST alone or GST fused to Hsc70 residues 1–540, 373–650, 373–540, or 540–650. The GST fusion proteins were captured by glutathione-Sepharose beads and analyzed by immunoblot with the TH antibody. As seen in Fig. 4*B*, *top left panel*, strong TH immunoreactive bands were present in the samples incubated with residues 540–650, whereas a slightly weaker band was present in the samples incubated with residues 373–540. Additional immunoblot analysis of these samples using anti-AADC antibody revealed that AADC preferentially precipitated with residues 373–540 and, to a much smaller degree, with residues 373–650 and 540–650 (Fig. 4*B*, *second panel*). These interactions were considered specific because no immunoreactive bands were detected in the GST-only samples. As a negative control, we also tested whether any of the GST fusion proteins containing different Hsc70 domains were able to pull down GS. No GS-immunoreactive bands were detected in any of our pulldown samples (Fig. 4*B*, *third panel*), demonstrating the specificity of the interaction between the Hsc70 fragments and TH and AADC. We repeated these pulldown experiments in rat striatum lysate. As seen in Fig. 4*B*, *right panels*, our results obtained from immunoblot analysis of the pulldowns performed in rat striatum lysate echoed those from the experiments using MN9D lysate. Specifically, TH was observed to interact strongly with 540–650 and, to a lesser degree, with 373–540, whereas AADC was noted to precipitate mainly with 373–540 and, at lower levels, with 373–650 and 540–650. Analysis of all samples with the GS antibody produced no detectable bands, and GST-only failed to pull down

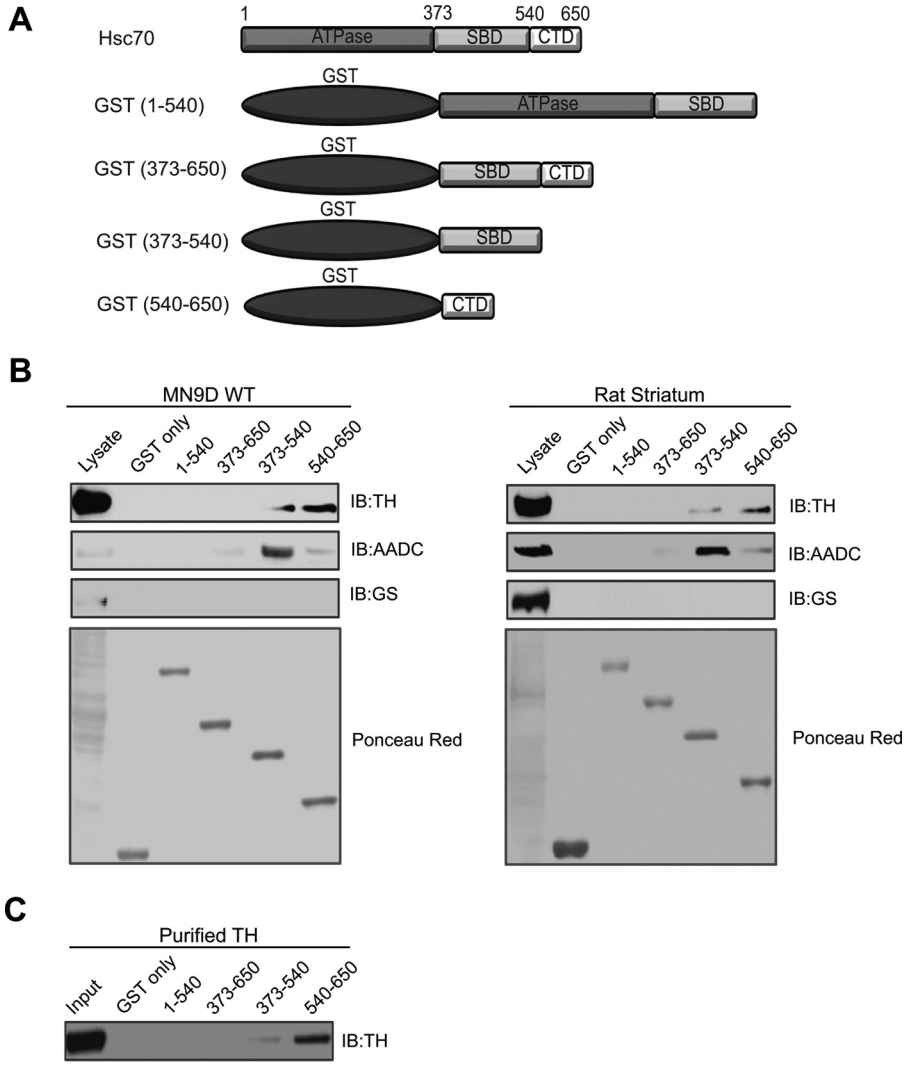

FIGURE 4. **SBD and CTD domains of Hsc70 interact with TH.** *A*, schematic of Hsc70 and GST fusion proteins containing three functional domains: the nuclear binding domain (*ATPase*, residues 1–373), SBD (residues 373–540), and CBD (residues 540–650). *B*, even amounts of immobilized GST fusion proteins were used for pulldown experiments in MN9D cell and rat brain lysates. Samples were analyzed by SDS-PAGE and IB with antibodies against TH (*first panel*) and AADC (*second panel*). As a negative control, the pulldown samples were also analyzed using the unrelated GS antibody (*third panel*). Ponceau red staining (*fourth panel*) shows even loading of the fusion proteins. *C*, *in vitro* binding assays were performed by incubating purified His_6-TH with even amounts of the Hsc70 GST fusion proteins or GST-only prior to SDS-PAGE and IB analysis using anti-TH antibody.

TH and AADC, again confirming the specificity of the interaction between the SBD and CTD of Hsc70, TH, and AADC.

To distinguish whether the Hsc70/TH interaction occurs via a direct protein-protein interaction or, alternatively, indirectly through the involvement of additional proteins, we next performed *in vitro* binding assays with purified TH. Here the Hsc70 GST fusion proteins or GST-only were incubated with a purified His_6-TH protein. Immunoblot analysis of pulldown samples demonstrated that TH co-precipitated predominantly with residues 540–650 and, at a much lower level, with 373–540 (Fig. 4*C*). No immunoreactive bands were detected in the control experiments using GST-only. These results not only recapitulate our findings in the GST pulldown experiments but also provide evidence demonstrating that the SBD and CTD of Hsc70 can directly bind TH.

Hsc70 Increases TH Activity in MN9D Cells and Purified Synaptic Vesicles from Brain—To test the functional consequences of the Hsc70-TH interaction, we next assessed the effect of Hsc70 on TH activity within a purified pool of synaptic vesicles (SVs) from mouse brain. We reported previously that purified VMAT2-expressing SVs obtained from mouse brain contain functional TH and AADC (18). Here TH activity of the SV preparation was determined in the presence or absence of 10 μg of recombinant Hsc70. The SVs incubated with Hsc70 displayed an ~70% increase in TH activity relative to SVs alone (Fig. 5*A*). TH activity within the SV fraction remained unaltered in the presence of Hsp70, Hsp60, or the denatured Hsc70 and Hsp70, suggesting that the Hsc70 effect on TH activity was specific. In additional experiments, we incubated purified SVs with increasing concentrations of recombinant Hsc70. Indeed, TH activity within the SV pool increased in an Hsc70 dose-dependent manner (Fig. 5*B*). Finally, because our pulldown assays indicate that the SBD and CTD of Hsc70 participate in the interaction with TH, we next examined whether these domains were sufficient to increase TH activity. We incubated SVs with the Hsc70 GST fusion proteins or GST-only prior to measuring

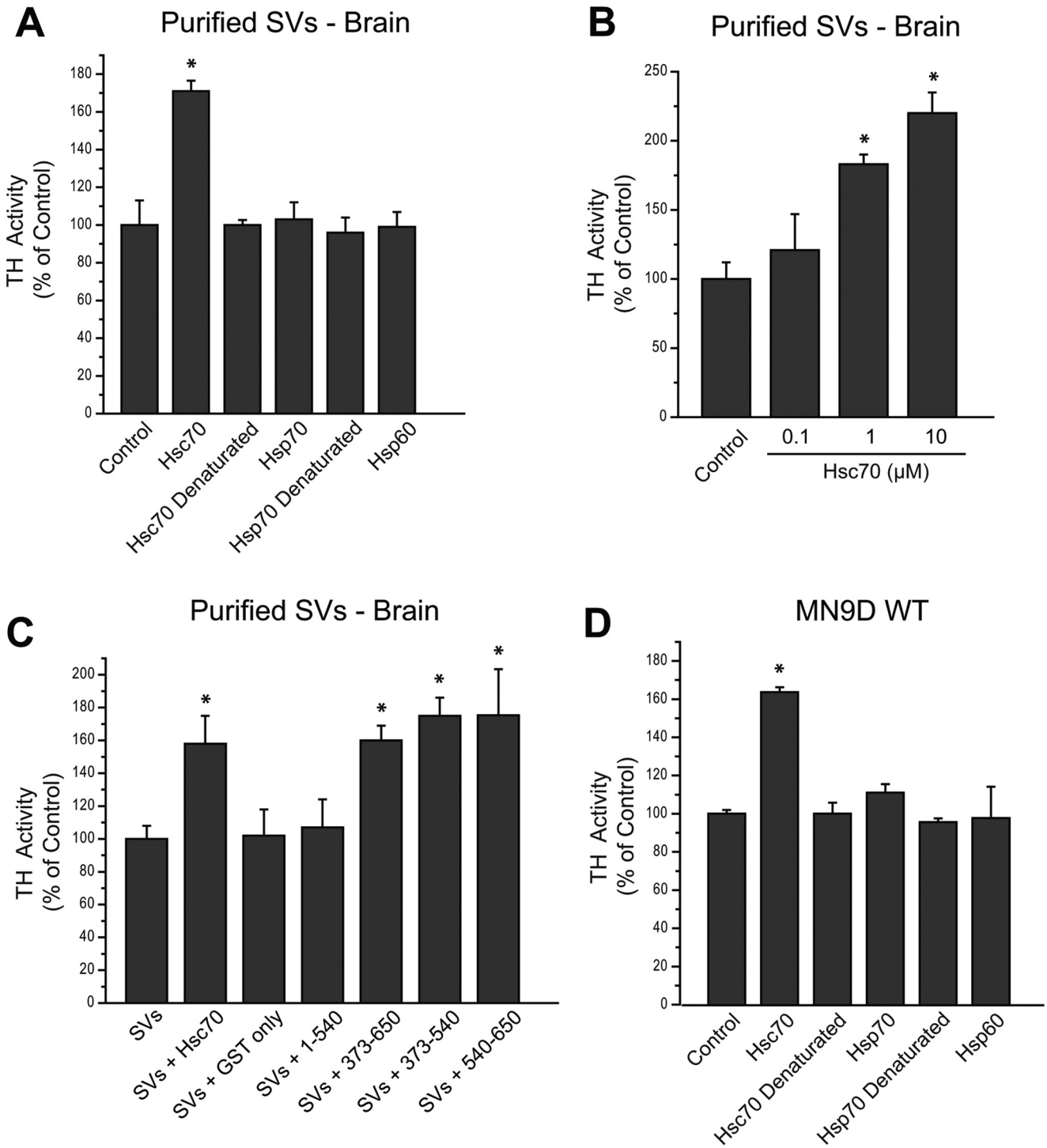

FIGURE 5. **Exogenous Hsc70 increases TH activity in MN9D cells and purified synaptic vesicles.** *A*, TH activity was measured in purified SVs obtained from mouse brain. The SVs were incubated with 10 μg of recombinant Hsc70, the closely related recombinant Hsp70 or Hsp60, or denatured Hsc70 or denatured Hsp70. The TH activity within the purified SV2 without recombinant protein (*Control*) was considered 100%. *B*, purified SVs were incubated without (*Control*) or with 0.1, 1, or 10 μM recombinant Hsc70. TH activity increased in a dose-dependent manner in the presence of recombinant Hsc70. *C*, TH activity was also assessed in the purified SVs in the presence of GST-only or GST-Hsc70 constructs. The GST-Hsc70 fusion constructs that interact with TH and AADC (*GST-373–650*, *GST-373–540*, and *GST-540–650*) were able to enhance TH activity in comparison with the TH activity in purified SVs alone (control, considered 100%). In contrast, non-interacting GST-Hsc70 fusion constructs (*GST-1–540*) did not alter TH activity. Recombinant Hsc70 was used as a positive control, and GST-only was used as a negative control. *D*, TH activity was assessed post-nuclear preparation from MN9D WT cells. The PNS was incubated with recombinant Hsc70, the closely related recombinant Hsp70 or Hsp60, or denatured Hsc70 or denatured Hsp70. The TH activity within the PNS alone in the control was considered 100%. *, $p < 0.05$.

TH activity. As seen in Fig. 5*C*, SVs incubated with GST fusion proteins containing residues 373–650, 373–540, or 540–650 displayed an ~60–70% increase in TH activity compared with that present in SVs alone. This increase was similar to that produced by incubation of the SVs with 10 μg of full-length recombinant Hsc70. On the other hand, GST-only and the

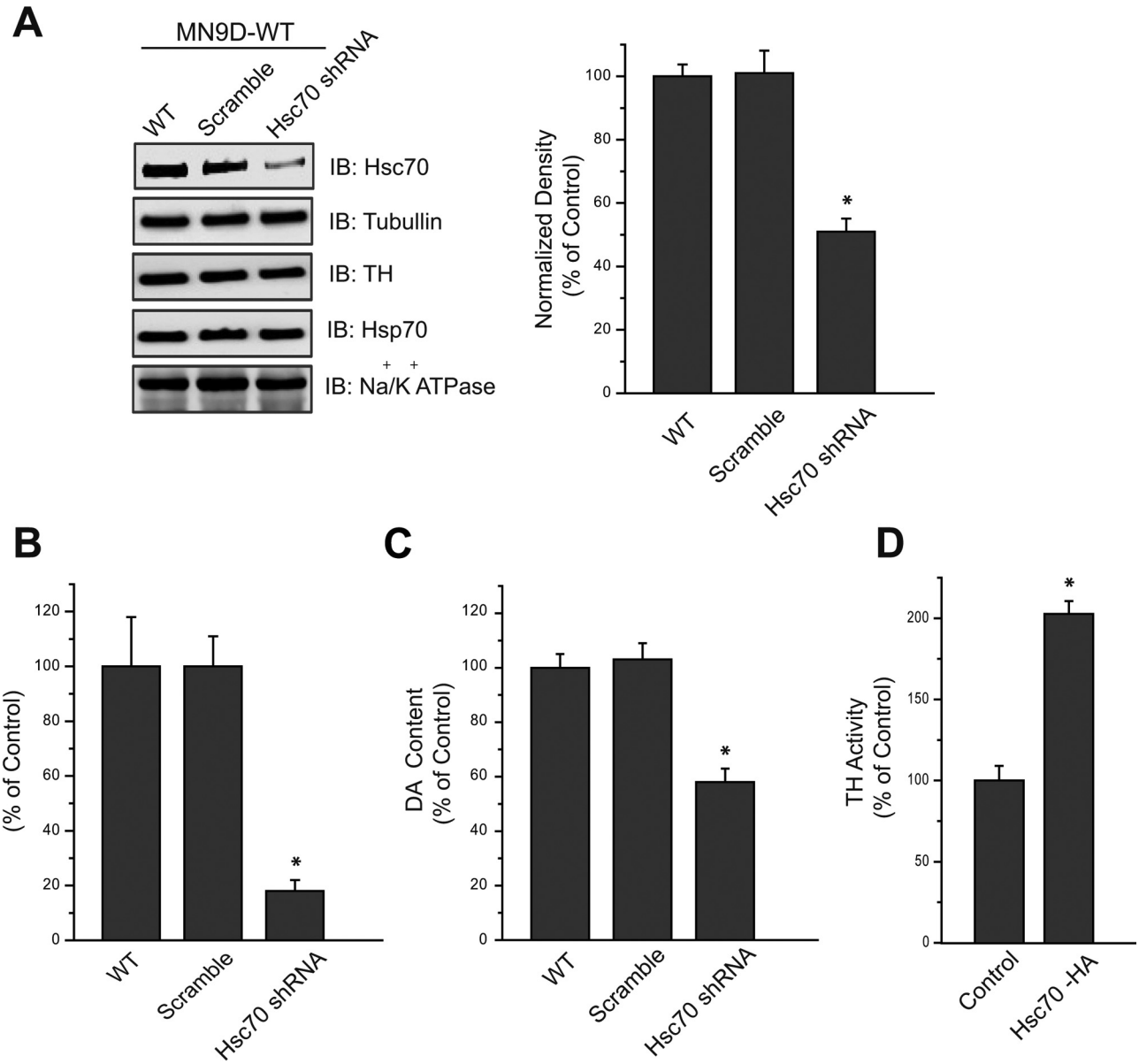

FIGURE 6. **Hsc70 expression affects TH activity and intracellular DA concentrations in MN9D cells.** *A*, representative IBs and densitometry analysis of MN9D cells, WT or stably transfected with scramble shRNA (*Scr*) or Hsc70 shRNA. Hsc70 expression was reduced in Hsc70 shRNA MN9D cells by ~50%, whereas TH, Hsp70, and sodium/potassium ATPase expression was not significantly altered. Densitometry analysis of Hsc70 expression was normalized to arbitrary densitometry units of α-tubulin and expressed as a percentage of Hsc70 expression in MN9D WT cells. *B*, TH activity was examined in the PNS of these samples. The Hsc70 shRNA MN9D cells exhibited an ~80% reduction in TH activity compared with WT and scramble shRNA stably transfected cells. *C*, intracellular DA levels present in the PNS of these samples were measured by HPLC. The DA levels present in the Hsc70 shRNA cells were reduced by ~40% compared with WT and scramble shRNA MN9D cells. *D*, in contrast, transfection of MN9D cells with Hsc70-HA resulted in increased TH activity compared with MN9D WT cells (*Control*). *, $p < 0.05$.

1–540 fragment of Hsc70 produced no significant changes in TH activity.

In a similar manner, TH activity was assessed in a post-nuclear preparation (PNS) from MN9D WT cells. As seen in Fig. 5*D*, TH activity was increased by ~60% when incubated with 10 μg of recombinant Hsc70 compared with the TH activity present in the MN9D PNS control. There was no effect on TH activity when Hsc70 was denatured prior to incubation or when the MN9D PNS was incubated with the closely related Hsp70 or Hsp60 (Fig. 5*D*), confirming the specificity of the Hsc70 effect on TH activity. These studies provided the first data indicating that the Hsc70/TH interaction modulates TH activity.

Hsc70 Expression Affects TH Activity and DA Content in MN9D Cells—Having demonstrated that exogenous Hsc70 is capable of modulating TH activity, we next examined whether changes in endogenous Hsc70 expression also produced similar functional results. To do this, we first generated a stable cell line in which Hsc70 expression was reduced by shRNA. Overexpression of an shRNA construct against Hsc70 mRNA in MN9D cells resulted in an ~50% reduction in Hsc70 protein levels compared with mock-transfected cells or those overexpressing a scramble shRNA (Fig. 6*A*). Tubulin, TH, Hsp70 (induced by heat shock), and Na^+/K^+-ATPase expression were not affected by the Hsc70 shRNA in these cells. We next examined whether TH activity and total DA content were altered in

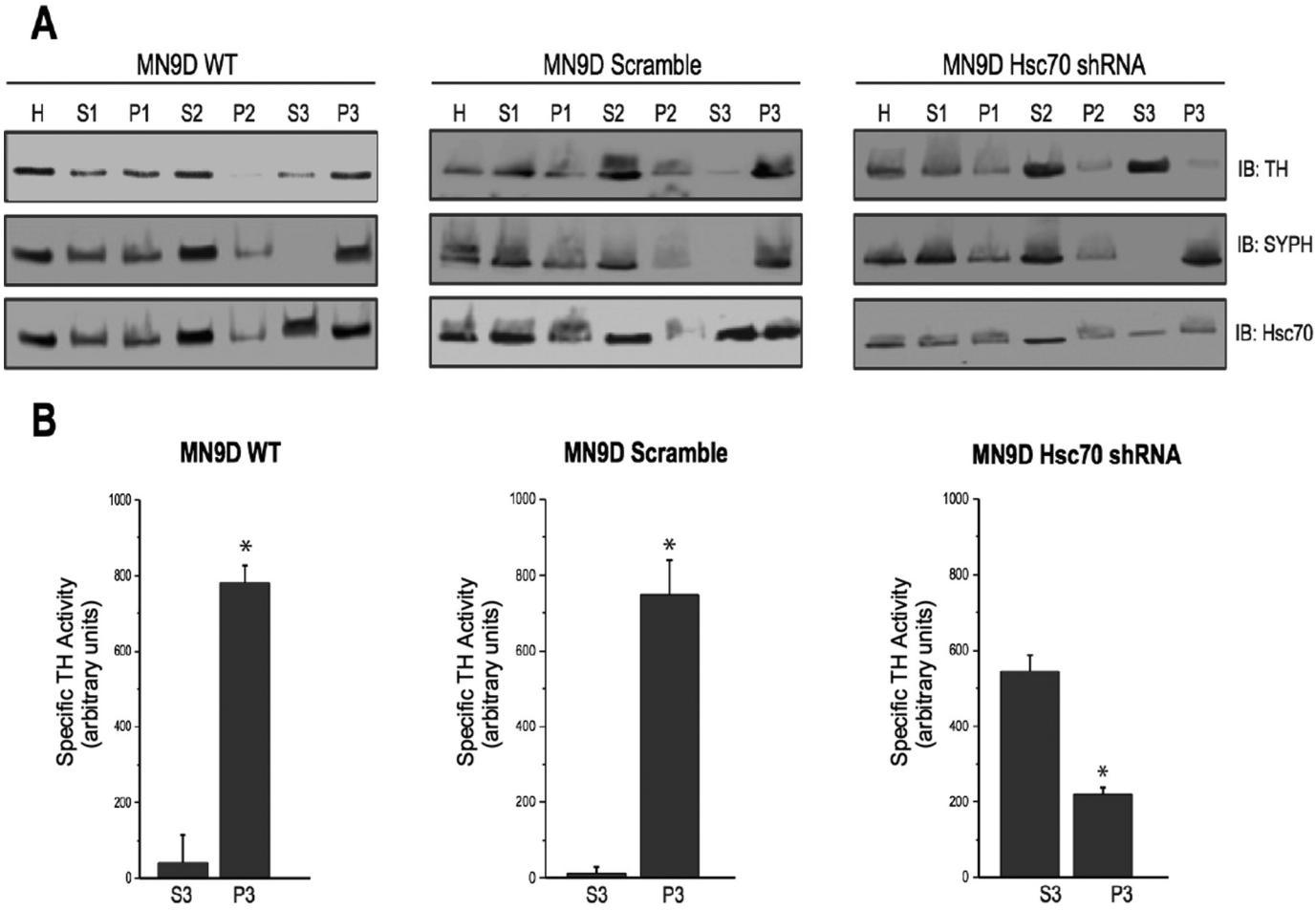

FIGURE 7. **Hsc70 expression affects the subcellular distribution of TH in MN9D cells.** *A*, an enriched SV preparation was prepared from WT, scramble shRNA, and Hsc70 shRNA cells by differential centrifugation. 50 μg of total protein from the original homogenate (*H*) as well as the supernatants (*S*) and pellets (*P*) from each step were analyzed by SDS-PAGE and IB using TH, SYPH, and Hsc70 antibodies. SYPH expression was enriched in the P3 sample compared with H and S3 of all three cell lines, confirming that the P3 sample represented enriched SVs. Consistent with our previous studies, TH expression was found in P3 of WT and scr-shRNA cells. Interestingly, this TH localization is shifted from P3 to S3 in Hsc70 shRNA cells. *B*, specific TH activity was examined in the S3 and P3 fractions of MN9D WT cells (*left panel*), MN9D cells expressing the scr-shRNA (*center panels*), and MN9D cells expressing the Hsc70 shRNA (*left panels*). *, $p < 0.05$.

these Hsc70 shRNA cells. Indeed, TH activity was reduced by ~80% in MN9D cells overexpressing the Hsc70 shRNA (Fig. 6*B*). This large decrease in TH activity is especially noteworthy in light of the fact that Hsc70 expression was decreased by only 50% by shRNA. In additional experiments, we also measured cellular DA content by HPLC. MN9D cells overexpressing the Hsc70 shRNA contained ~40% less DA compared with WT or scramble MN9D cells (Fig. 6*C*). Having observed the effect of reducing Hsc70 levels on both TH activity and DA content, it was next important to consider whether increased Hsc70 expression resulted in increased TH activity. Thus, we overexpressed Hsc70 in MN9D cells by transiently transfecting them with an HA-tagged Hsc70 construct. The Hsc70-HA transfected cells exhibited nearly twice the amount of TH activity displayed by MN9D WT cells (Fig. 6*D*). These data are consistent with our previous data examining the effects of recombinant Hsc70 and support the notion that Hsc70 modulates TH activity.

Hsc70 Affects the Subcellular Localization of TH in MN9D Cells—In previous reports, we have demonstrated that TH expression and activity are enriched in SV preparations. However, the mechanism by which TH is targeted to synaptic vesicles remains unknown. We next examined whether Hsc70 might be involved in targeting TH to SVs by examining TH levels in an enriched SV preparation (P3) from MN9D cells overexpressing Hsc70 shRNA. Each step within this process was analyzed by immunoblot using antibodies against TH, Hsc70, and the synaptic vesicle marker SYPH. As shown in Fig. 7*A*, *left panel*, TH and Hsc70 co-fractionated with SYPH in WT MN9D cells, confirming localization to SVs. Immunoblotting analysis of the scramble shRNA MN9D cells revealed no significant changes in expression of TH, Hsc70, or SYPH throughout the fractionation process (Fig. 7*A*, *left* and *center panels*). In addition, activity assays demonstrated that most of the TH activity was recovered in P3 samples in MN9D WT cells and cells expressing the scramble shRNA (Fig. 7*B*, *left* and *center panels*). However, when examining MN9D cells overexpressing Hsc70 shRNA, marked differences in TH fractionation and activity pattern were detected. Specifically, TH immunoreactivity within SV preparation P3 was diminished and, instead, enriched within the soluble S3 fraction (Fig. 7*A*, *right panel*). Similarly, TH activity was increased in the S3 fraction, with a concomitant decreased in the vesicular P3 fraction (Fig. 7*B*, *left panel*). The fractionation pattern of

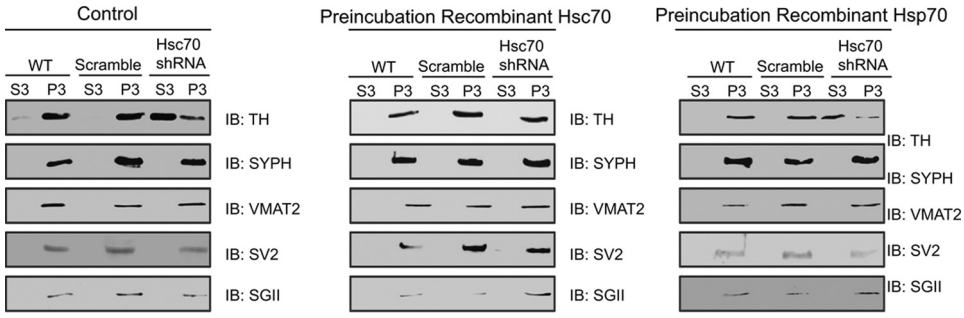

FIGURE 8. **Recombinant Hsc70 is capable of restoring TH levels at the synaptic vesicle in Hsc70-shRNA cells.** The synaptic vesicle fractionations were repeated under conditions where S2 was incubated alone (*Control*) or in combination with either recombinant Hsp70 or Hsc70 prior to obtaining S3 and P3. 50 μg of total proteins from H, S3, and P3 of WT, scramble shRNA, and Hsc70 shRNA MN9D cells were analyzed by SDS-PAGE and IB. Again, TH was enriched in P3 of WT and scramble shRNA cells in S3 of the Hsc70 shRNA cells under normal conditions. Importantly, incubation with Hsc70 restored TH levels to the P3 fraction in Hsc70 shRNA cells. Incubation with the closely related Hsp70 protein had no effect on TH distribution, confirming the specificity of the Hsc70 effect. IB analysis with SYPH, VMAT2, SV2, and secretogranin II antibodies confirmed that the fraction P3 contained synaptic vesicles.

SYPH remained unchanged, ruling out a nonspecific effect of Hsc70 knockdown on the fractionation of SVs. These results suggest that Hsc70 influences the localization of TH to synaptic vesicles.

To provide more direct evidence for a role of Hsc70 in TH localization to SVs, we next examined whether the addition of exogenous Hsc70 rescued the effects of knocking down Hsc70. We incubated S2, the supernatant that was centrifuged one final time prior to yielding the enriched SV preparation, with or without the addition of exogenous Hsc70 or the closely related Hsp70. We then analyzed the final supernatant (S3) and the pellet containing the enriched SV fraction P3 by immunoblot using TH, SYPH, VMAT2, SV2, and secretogranin II antibodies. Consistent with our previous findings, WT and scramble shRNA MN9D samples displayed enriched TH levels in P3 compared with S3, whereas Hsc70 shRNA cells showed higher levels of TH in the S3 as opposed to the P3 fraction (Fig. 8, *left panel*). More importantly, the addition of recombinant Hsc70 to the S2 of the Hsc70 shRNA samples restored levels of TH at the SV-enriched P3 preparation (Fig. 8, *center panel*). In contrast, exogenous Hsp70 did not restore TH levels in the P3 samples from Hsc70 shRNA cells (Fig. 8, *right panel*), demonstrating the specificity of the Hsc70 effect. The expression of the SV markers SYPH, VMAT2, SV2, and secretogranin II was not altered by incubation with either Hsc70 or Hsp70 or any of the shRNA manipulations. Taken together, these findings support a role for Hsc70 in the regulation of TH activity and targeting to synaptic vesicles.

Discussion

Our findings consistently support a role for Hsc70 in the presynaptic control of DA homeostasis. It is well known that TH exists in two distinct forms: soluble or bound to synaptic vesicles at presynaptic terminals. The association of TH with synaptic vesicle membranes would place the enzyme in a specific microdomain where synthesized DA would be rapidly transported into synaptic vesicles through VMAT2 (18). This close proximity between TH and VMAT2 would ensure efficient coordination and regulation of DA synthesis, storage, and release. However, the mechanism whereby TH is targeted to the synaptic vesicle membrane has remained elusive. Here we provide evidence for a novel interaction between Hsc70 and TH that regulates the activity and localization of TH to synaptic vesicles. We present several lines of biochemical and functional evidence supporting a physical and functional interaction between Hsc70 and TH. First, Hsc70 and TH co-precipitate from dopaminergic MN9D cells or rat brain striata. Second, GST pulldown assays confirmed this interaction, identified the SBD and CTD domains of Hsc70 as the interacting regions, and demonstrated the ability of Hsc70 and TH to interact directly. Third, immunocytochemical assays verified that Hsc70 and TH co-localize in midbrain dopaminergic neurons *in vivo* and *in vitro*. Fourth, TH activity from purified synaptic vesicles increased in a dose-dependent manner in the presence of either recombinant Hsc70 or GST fusion proteins containing the SBD or CTD of Hsc70. Fifth, down-regulation of Hsc70 in MN9D cells resulted in decreased TH activity and DA content, whereas Hsc70 overexpression increased TH activity. Finally, fractionation experiments revealed that Hsc70 expression affects the localization of TH to synaptic vesicles in MN9D cells. Collectively, these results provide compelling evidence of a novel interaction between Hsc70 and TH that regulates the activity and the localization of TH to SVs, suggesting a novel role for Hsc70 in the regulation of DA homeostasis.

Heat shock proteins are ubiquitously expressed molecular chaperones. The Hsp70 family includes the stress-inducible Hsp70 (also termed Hsp72/Hsp701A) as well as the constitutively expressed Hsc70 (also termed Hsp73/Hsp701B). Both Hsp70 and Hsc70 contain three functional domains: the nuclear binding (NBD-ATPase) domain, the SBD, and the CTD. They are 85% identical at the amino acid level. Despite this shared homology, our data indicate that the interaction and regulation of TH is Hsc70-specific. TH co-precipitated with Hsc70 but not Hsp70. Furthermore, our functional assays also showed that recombinant Hsp70 failed to produce changes in the activity or subcellular localization of TH that were associated with Hsc70. These results may not be surprising in light of the stress-inducible nature of Hsp70 *versus* the constitutive nature of Hsc70. One can imagine that the modulation of DA synthesis demands persistent and sustained control, which may not be afforded by the transiently expressed Hsp70 but would necessitate a protein that is constitutively and widely expressed, such as Hsc70.

Traditionally, Hsc70 has been reported to have roles in a variety of cellular functions, including protein folding, assembly, targeting, transport, and degradation (19, 20). Many of the roles that Hsc70 plays in protein homeostasis have been well described, but recent studies are identifying a growing number of protein partners and are consequently revealing novel functions associated with heat shock proteins. For example, several reports have identified protein-protein interactions between members of the Hsp70 family and membrane signaling proteins, including the transferrin receptor (21), the aquaporin channel (22), the chloride channel ClC-2 (23), and melanocortin receptor 4 (24). Likewise, an increasing number of proteins that influence brain function have been identified to interact with heat shock proteins. In presynaptic terminals, Hsc70 forms a complex with cysteine string protein and small glutamine-rich tetratricopeptide repeat domain protein that plays an important role in synaptic vesicle uncoating during clathrin-dependent endocytosis (25–27). Hsc70 also binds gephyrin, induces gephyrin clustering, and regulates the formation of tertiary complexes, including GABA and glycine receptors, at inhibitory synapses (28). These studies support an emerging and important role for Hsc70 in the regulation of presynaptic function.

Our data support a mechanism in which Hsc70 facilitates efficient coupling of DA synthesis and storage systems by localizing TH to the synaptic vesicle where the enzyme can interact with VMAT2. This mechanism is supported by our data showing that down-regulation of Hsc70 by shRNA resulted in decreased levels and activity of TH associated with synaptic vesicles and lower intracellular DA levels. Interestingly, a recent study in *Drosophila* identified a physical and functional interaction between TH and GTP-cyclohydrolase I (GCH1), an enzyme that is responsible for synthesis of the DA co-factor tetrahydrobiopterin (29). Similarly, Hsc70 has also been described as a GCH1-interacting protein using a yeast two-hybrid system (30). Although these studies did not explore the subcellular location of the GCH1 interactions, it is tempting to speculate that GCH1 also participates in the Hsc70-TH-AADC-VMAT2 complex as a critical enzyme necessary for DA synthesis. More recently, a functional interaction between VMAT2 and the DA biosynthetic complex through the *Catecolamines up (Catsup*) gene was identified in *Drosophila* DA neurons (31). A complex network of proteins linking DA synthesis and synaptic vesicle refilling might require highly regulated mechanistic steps involving assembly/disassembly and conformational changes that promote correct protein folding, localization, and activity. We propose that Hsc70 plays a crucial role in organizing the DA synthesis-refilling complex.

A similar coupling mechanism between synthesis and storage has been described in the GABA system. Specifically, the vesicular GABA transporter was reported to associate with the enzyme responsible for GABA synthesis, glutamic acid decarboxylase (GAD65), at synaptic vesicles (32). This association involved a multiprotein complex involving Hsc70 as well as calmodulin-dependent kinase and cysteine string protein (33). Hsc70 was proposed to anchor GAD65 to the synaptic vesicle, where it subsequently complexes with the vesicular GABA transporter and the other proteins. Thus, it seems that Hsc70 plays a crucial role in neurotransmitter homeostasis within both the GABA and DA systems. In both cases, Hsc70 localizes the synthesis enzymes to be in proximity to the vesicular transporter, allowing neurotransmitter synthesis to occur at the synaptic vesicle membrane junction, where it is coupled with vesicular transport and storage within the synaptic vesicles.

Neurotransmitter homeostasis requires the fine control and regulation of several mechanisms, including synthesis, vesicular refilling, release, reuptake, and degradation. Within the dopamine system, these mechanisms interact to ensure that cytosolic DA levels remain low and that its potentially toxic effects are minimized. Indeed, cytosolic concentrations of DA in the substantia nigra are practically undetectable (34). Increased metabolism of DA leads to toxicity caused by the generation of reactive species such as $OH^{\cdot}$, O_2^{-}, H_2O_2, and neurotoxic quinines (35–38). Indeed, chronic exposure to cytosolic DA may elicit progressive degeneration of DA-containing neurons in the substantia nigra pars compacta. Significant loss of dopaminergic neurons is associated with deficient striatal dopamine levels and, consequently, the clinical manifestations of Parkinson disease (39–42). Our data suggests a biochemical complex involving VMAT2, Hsc70, and TH/AADC that couples DA synthesis and synaptic vesicle storage, which would limit DA levels to the synaptic vesicle microenvironment, thereby minimizing cytosolic dopamine levels and its toxic effects. Future studies will be required to examine how disruption of these mechanisms leads to toxicity and potential neurodegeneration.

Experimental Procedures

Reagents—Male Sprague-Dawley rats (350 g) between 8 and 10 weeks old were obtained from Hilltop Lab Animals, Inc. (Scottdale, PA). The antibodies against VMAT2 (AB1598P), TH, AADC, Na^+/K^+-ATPase, GS, and GAD67 as well as the nonspecific IgGs from goat (PP40) and rabbit (PP64) were from Millipore (Billerica, MA). The antibody against synaptophysin was obtained from BD Transduction Laboratories, and the SV2 antibody was from Synaptic Systems (Göttingen, Germany). The Hsp70, Hsc70, and Grp78 antibodies were supplied by Assay Design (Ann Arbor, MI), and the HSP90 antibody was from Cell Signaling Technology (Danvers, MA). Secondary antibodies conjugated with HRP were from Jackson ImmunoResearch Laboratories (West Grove, PA), and secondary antibodies conjugated with Alexa Fluor 488 and 555 were from Molecular Probes, Invitrogen. Purified recombinant Hsc70, Hsp70, Hsp60, and Hsc70 (1–386)-ATPase fragments were supplied by Assay Designs. All other reagents were from Sigma-Aldrich (St. Louis, MO) unless stated otherwise.

Cell Culture—MN9D cells were provided by Dr. Alfred Heller (University of Chicago) and maintained in high-glucose DMEM supplemented with 10% FBS and 50 μg/ml each penicillin and streptomycin and maintained at 37 °C in a humidified 5% CO_2 incubator. In some cases, cells were transfected with 10 μg of DNA using Transfectin (Bio-Rad) according to the recommendations of the manufacturer. Transfected cells were allowed to grow for an additional 48 h prior to further studies.

Heat Shock Experiments—Culture dishes containing MN9D cells were transferred for heating into a 42 °C incubator for 5 h

and subsequently returned for recovery in a 37 °C incubator for 17 h, both with 5% CO_2. Cell lysates were analyzed by 10% SDS-PAGE and immunoblot.

Generation of Stable Knockdown Clones—HuSH 29-mer shRNA constructs against Hsc70 (shRNA-Hsc70) were obtained from OriGene Technologies (Rockville, MD). The small hairpin RNA sequences were 5′-GGTAACCGCACCAC-GCCAAGCTATGTTGC-3′, 5′-TGAGGAGTTGAATGCTG-ACCTGTTCCGTG-3′, 5′-CAGGCAGCCATTCTATCTGG-AGACAAGTC-3′, and 5′-GAACTCACTGGAGTCCTATG-CCTTCAACA-3′. Control cells were transfected with the same vector expressing a scramble short hairpin RNA sequence (scr-shRNA). MN9D cells were transfected with the shRNA-Hsc70 or scr-shRNA constructs using Lipofectamine 2000 (Invitrogen) according to the recommendations of the manufacturer, and a final concentration of 2.5 μg/μl puromycin was maintained in the medium 24 h after transfection.

Preparation of Brain and MN9D Lysates—Rat striata were homogenized with a polytron in buffer A (20 mM HEPES (pH 7.4), 125 mM NaCl, and 1 mM EGTA) containing protease inhibitors (Pierce). Triton X-100 was added to a final concentration of 1%, and the samples were incubated with rotation for 1 h at 4 °C. Samples were centrifuged twice at 4 °C: first at 16,000 × *g* for 10 min and then at 20,000 × *g* for 60 min. The supernatant was collected, measured for protein concentration, and used in subsequent experiments. MN9D lysate was obtained using the same homogenization procedure but only subjected to one centrifugation at 16,000 × *g* for 10 min at 4 °C.

Immunoprecipitations—Anti-VMAT2 (1:200), anti-TH (1:200), control IgGs (1:200), or no antibody (beads only) were added to either striata or cell lysates and incubated with rotation for 1 h at 4 °C. Next, 50 μl of a mixture of protein A- and protein G-Sepharose beads (GE Healthcare) were added to all samples and incubated with rotation for an additional hour at 4 °C. Following centrifugation at 13,000 × *g* for 3 min, pellets were washed two times in buffer A containing 1% Triton X-100 and twice in PBS in the presence of protease inhibitors. The resulting pellets were resuspended in 30 μl of sample buffer containing 10% β-mercaptoethanol (β-ME) and incubated at 37 °C for 30 min prior to analysis using 10% SDS-PAGE and immunoblot.

Immunofluorescence—For midbrain sections, C57BL/6J mice (Jackson Laboratory; Bar Harbor, ME) were perfused with 10 ml of 0.1 M PBS followed by 30 ml of 4% paraformaldehyde in 0.1 M PBS. Brains were removed and cryoprotected in 30% sucrose in 10 mM PBS for 48 h before coronal sections (40 μm) were cut on a freezing microtome. Primary DA neurons in culture were prepared as described previously (43). Cultures were maintained at 37 °C in an atmosphere containing 5% CO_2 in equilibrium with H_2O. Following fixation, samples were blocked in 10% normal goat serum in 10 mM PBS with 0.3% Triton X-100 for 1 h at room temperature. Samples were then incubated overnight at 4 °C in primary antibodies (rat anti-HSC70 (1:500) and rabbit anti-TH (1:2000) in 10 mM PBS with 0.3% Triton X-100). Primary neurons were then exposed to the following secondary antibodies: goat anti-rabbit (1:500, Alexa Fluor 555) and goat anti-rat (1:500, Alexa Fluor 488). Brain sections were exposed to the same primary antibodies and then incubated with goat anti-rabbit (1:500, Alexa Fluor 488) and goat anti-rat (1:500, Alexa Fluor 555) secondary antibody fluorophores for 1 h at room temperature in 10 mM PBS with 0.3% Triton X-100. Sections were then washed, mounted, coverslipped with Fluoromount (MP Biomedicals, Irvine, CA) and examined using an Olympus Fluoview FV1000 confocal unit fitted to an Olympus BX61 microscope (Olympus, Center Valley, PA).

GST Pulldown Assays—Hsc70-GST fusion protein constructs were generously provided by Dr. Ernst Ungewickell (Hannover Medical School, Hannover, Germany) and contained portions of bovine Hsc70. The GST-Hsc70 fusion proteins were designated by the amino acid residue contained in each construct: 1–540, 373–540, 373–650, or 540–650 (44). *Escherichia coli* BL-21 was transformed with the different pGEX constructs, grown at 37 °C to an optical density between 0.4–0.7, incubated with 0.1–1 mM isopropyl 1-thio-β-D-galactopyranoside for 2–4 h at 37 °C, and harvested by centrifugation at 4300 × *g* for 10 min. All GST fusion proteins were purified from cleared lysate by standard affinity chromatography using glutathione-Sepharose 4B beads (GE Healthcare) as recommended by the manufacturer. For pulldown experiments from rat brain striatum or MN9D cell lysates, even amounts of the immobilized Hsc70 GST fusion proteins or GST-only were incubated overnight at 4 °C. The GST fusion proteins were then immobilized by incubating the samples with 50 μl of pre-equilibrated glutathione-Sepharose 4B beads for 30 min at 4 °C. All samples were washed three times with buffer containing 50 mM Tris and 300 mM NaCl (pH 8.0) for 10 min. In both cases, the washed samples were suspended in 50 μl of protein sample buffer containing 10% β-ME and incubated at 37 °C for 30 min prior to analysis using 10% SDS-PAGE and immunoblot.

Purification of Recombinant His_6-TH—TH subcloned into the pQE30 vector for prokaryotic expression of the His_6 tag was a kind gift from Dr. Janis O'Donnell (University of Alabama). The DNA was used to transform competent M15 bacterial cells and purified with nickel-nitrilotriacetic acid superflow columns (Qiagen, Valencia, CA) according to the protocols of Funderburk *et al.* (45).

In Vitro Binding Assay—50 μg of recombinant His_6-TH and 50 μg of purified Hsc70 GST-fused proteins 1–540, 373–540, 373–650, 540–650, or GST-only were diluted in 400 μl of buffer A. Following 1 h incubation at room temperature with rotation, 50 μl of the glutathione-Sepharose 4B beads was added and incubated for another 3 h at room temperature with rotation. The beads were washed three times with cold PBS containing 1% Triton X-100 (pH 7.65) for 1 min. 50 μl of sample buffer containing 10% β-ME was added to the washed beads and incubated at 37 °C for 30 min to release bound proteins prior to Western blotting analysis.

Purification of Synaptic Vesicles from Brain—To obtain a pure synaptic vesicle pool from brain tissue, we isolated vesicles based on the protocol described by Morciano *et al.* (46) and Egaña *et al.* (47). Briefly, whole brain from rat was homogenized with 20 strokes in a glass Teflon homogenizer in 10 volumes of 0.32 M sucrose, 5 mM Tris/HCl (pH 7.4) supplemented with protease inhibitors. The homogenate was centrifuged at 1000 × *g* for 10 min at 4 °C. The resulting pellet was discarded, and the

entire supernatant was layered on top of a discontinuous Percoll gradient prepared using three different layers of Percoll solutions (3%, 10%, and 23% (v/v)) diluted in the original homogenization buffer. The Percoll gradient was centrifuged at 31,400 × *g* for 20 min at 4 °C, and the turbid fraction was collected, containing isolated synaptosomes. Four volumes of the original homogenization buffer were added to the synaptosomes, and the sample was centrifuged again at 20,000 × *g* for 1 h at 4 °C. The resulting pellet was hypo-osmotically lysed in 6.5 ml of 5 mM Tris-HCl (pH 7.4) by pipetting the sample up and down 20 times and passing the sample through both 22- and 27.5-gauge needles. This suspension was centrifuged at 188,000 × *g* for 2 h at 4 °C. The resulting pellet was resuspended in 0.5 ml of sucrose buffer (200 mM sucrose, 0.1 mM $MgCl_2$, 0.5 mM EGTA, and 10 mM HEPES (pH 7.4)) and layered onto a discontinuous sucrose gradient ranging from 0.3–1.2 M sucrose (both prepared in 10 mM HEPES and 0.5 mM EGTA (pH 7.4)). The sucrose gradient was centrifuged at 85,000 × *g* for 2 h at 4 °C, and 500-μl fractions were collected from top to bottom and analyzed using Western blotting.

Postnuclear Supernatant Preparation—Medium was removed from 10-cm plates of MN9D cells. After rinsing the plates with PBS, cells were scraped from dishes and pelleted at 305 × *g* for 3 min. The resulting pellet was resuspended in buffer B (320 mM sucrose, 0.1 mM $MgCl_2$, 0.5 mM EGTA, and 10 mM HEPES (pH 7.4)) containing protease inhibitors. The pellet was homogenized using 25 strokes with a Wheaton homogenizer (Wheaton Science Products, Millville, NJ), followed by 25 passages through a 25-gauge needle. The sample was centrifuged at 1000 × *g* for 2 h at 4 °C, resulting in the postnuclear supernatant (PNS).

Subcellular Fractionation of MN9D Cells—Medium was removed from confluent 10-cm plates of MN9D cells. After rinsing the plate with PBS, cells were scraped from dishes and pelleted at 305 × *g* for 3 min. The resulting pellet was resuspended in buffer B containing protease inhibitors. After homogenization using 25 strokes in a Wheaton homogenizer followed by 25 passages through a 25-gauge needle, the sample was centrifuged at 1000 × *g* for 5 min at 4 °C to remove nuclei and cellular debris (P1). The resulting supernatant (S1) was centrifuged at 27,000 × *g* for 35 min, resulting in S2 and P2. A final centrifugation of S2 at 180,000 × *g* for 2 h at 4 °C yielded S3 and P3. As shown by Parra *et al.* (48), the resulting pellet contained an enriched synaptic vesicle fraction and was called P3. In some cases, the S2 fraction was incubated for 1 h with a final concentration of 1 μM of either recombinant Hsc70 or recombinant Hsp70 prior to the final centrifugation. In all cases, the pellets and supernatants were analyzed using Western blotting.

Western Blotting Analysis—Samples containing 10% β-ME were incubated at 37 °C for 30 min, separated by SDS-PAGE on 10% Tris-HCl polyacrylamide gels, and transferred to nitrocellulose membranes using the Bio-Rad system. Lysates were used in all experiments as a positive control. Nitrocellulose membranes were first blocked for 1 h in TBS buffer (50 mM Tris-HCl, 150 mM NaCl, and 0.2% Tween 20) containing 5% dry milk, incubated with the indicated primary antibody for 1 h in blocking buffer, washed three times for 10 min, and incubated with an HRP-conjugated secondary antibody. Following all antibody incubations, membranes were washed three times with TBS buffer, and protein bands were visualized using the West Pico system (Pierce).

TH Activity—TH activity was measured according to Perez *et al.* (49), Reinhard *et al.* (50), and Cartier *et al.* (18). Using this assay, 1 mol of $[^3H]H_2O$ is generated for each 1 mol of [^{3}H]L-tyrosine that is converted to DOPA by TH and is therefore a direct measurement of TH activity. 100 μl of sample was added to an equal volume of 2× assay buffer to bring the final concentrations to 15 mM Tris maleate, 50 μM unlabeled L-tyrosine, 0.4 μCi/mmol [3,5-^{3}H]L-tyrosine, 5 mM ascorbate, 0.45 mg/ml catalase, 1 mM TH co-factor BH_4 (pH 6.8). Samples were incubated for 25 min at 37 °C, and reactions were stopped on ice. Released $[^3H]H_2O$ was separated from [^{3}H]L-tyrosine using 7.5% charcoal/HCl. Because BH_4 is an essential co-factor for TH activity, the nonspecific background was determined in the absence of BH_4. $[^3H]H_2O$ was then added to 4 ml of Biosafe II scintillation liquid, and radioactivity was counted in a Beckman LS 6500 scintillation counter (Beckman Coulter, Fullerton, CA). Specific TH activity was determined as the amount of $[^3H]H_2O$ generated per minute and normalized with the amount of total TH in the sample as measured by Western blotting.

Determination of DA Content—Perchloric acid (0.1 M) was added to confluent MN9D plates. Cells were harvested, homogenized, and centrifuged at 15,000 × *g* at 4 °C for 15 min. Supernatants were collected and transferred to 0.22-μm Durapore PVDF centrifugal filter units (Millipore, Ultrafree-MC) and centrifuged at 15,000 × *g* at 4 °C for 10 min for further purification. Samples were stored at −80 °C until assayed for DA, and its metabolites were coupled with electrochemical detection using HPLC. Aliquots (10–20 μl) of the supernatant were injected onto a C18 column (3 μm, 2 × 150 mm, ESA Inc., Chelmsford, MA) using a mobile phase consisting of 50 mM $H_2NaO_4P{\cdot}H_2O$, 0.72 mM sodium octyl sulfate, 0.075 mM Na_2EDTA, and 10% acetonitrile (v/v) (pH 3.0). The mobile phase was pumped through the system at 0.3 ml/min using an ESA 580 pump (ESA Inc.). Analytes were detected using an ESA Coulochem model 5100A detector, an ESA model 5010 conditioning cell, and an ESA model 5014B microdialysis cell (ESA, Inc.). The settings for detection were $E_1 = -150$ mV, $E_2 = +280$ mV, and guard cell = +350 mV. The limits of detection for DA were in the femtomole range. Detection for DA and its metabolites were identified relative to the retention times set to known standards.

Data Analysis—Results are presented as mean ± S.E. Significant differences between means were determined by Student's *t* test, with $p < 0.05$ considered statistically significant (*).

Author Contributions—G. E. T. conceived and coordinated the study and wrote the paper. L. A. P., T. B. B., and J. A. P. designed, performed, and analyzed the co-immunoprecipitation, fractionation, and TH activity experiments and wrote the paper. L. A. P., A. D. S., and M. J. Z. performed and analyzed the experiments involving DA levels. J. D. J. and R. K. L. performed and analyzed the experiments shown in Fig. 3. S. T. provided data analysis assistance. All authors reviewed the results and approved the final version of the manuscript.

Acknowledgments—We thank the members of the Torres laboratory for helpful discussions.

References

1. Skagerberg, G., Lindvall, O., and Björklund, A. (1984) Origin, course and termination of the mesohabenular dopamine pathway in the rat. *Brain Res.* **307,** 99–108
2. Björklund, A., and Dunnett, S. B. (2007) Dopamine neuron systems in the brain: an update. *Trends Neurosci.* **30,** 194–202
3. Arias-Carrion, O., and Poppel, E. (2007) Dopamine, learning, and reward-seeking behavior. *Acta Neurobiol. Exp.* **67,** 481–488
4. Greengard, P. (2001) The neurobiology of dopamine signaling. *Biosci. Rep.* **21,** 247–269
5. Carlsson, A. (1987) Development of new pharmacological approaches in Parkinson's disease. *Adv. Neurol.* **45,** 513–518
6. Roth, R. H., and Elsworth, J. D. (1995) in *Psychopharmacology: The Fourth Generation of Progress* (Bloom, F. E., and Kupfer, D. J., eds) pp. 227–243, Raven, New York
7. Koob, G. F., and Le Moal, M. (1997) Drug abuse: hedonic homeostatic dysregulation. *Science* **278,** 52–58
8. Adinoff, B. (2004) Neurobiologic processes in drug reward and addiction. *Harv. Rev. Psychiatry* **12,** 305–320
9. Zigmond, R. E., Schwarzschild, M. A., and Rittenhouse A. R. (1989) Acute regulation of tyrosine hydroxylase by nerve activity and by neurotransmitters via phosphorylation. *Annu. Rev. Neurosci.* **12,** 415–461
10. Haycock, J. W., and Haycock, D. A. (1991) Tyrosine hydroxylase in rat brain dopaminergic nerve terminals: multiple-site phosphorylation *in vivo* and in synaptosomes. *J. Biol. Chem.* **266,** 5650–5657
11. Christenson, J. G., Dairman, W., and Udenfriend, S. (1972) On the identity of DOPA decarboxylase and 5-hydroxytryptophan decarboxylase. *Proc. Natl. Acad. Sci. U.S.A.* **69,** 343–347
12. Fon, E. A., and Edwards R. H. (2001) Molecular mechanisms of neurotransmitter release. *Muscle Nerve* **24,** 581–601
13. Jones, S. R., Gainetdinov, R. R., Jaber, M., Giros, B., Wightman, R. M., and Caron, M. G. (1998) Profound neuronal plasticity in response to inactivation of the dopamine transporter. *Proc. Natl. Acad. Sci. U.S.A.* **95,** 4029–4034
14. Kopin, I. (1985) Catecholamine metabolism: basic aspects and clinical significance. *Pharmacol. Rev.* **37,** 333–364
15. Sager, J. J., and Torres, G. E. (2011) Proteins interacting with monoamine transporters: current state and future challenges. *Biochemistry* **50,** 7295–7310
16. Requena, D. F., Parra, L. A., Baust, T. B., Quiroz, M., Leak, R. K., Garcia-Olivares, J., and Torres, G. E. (2009) The molecular chaperone Hsc70 interacts with the vesicular monoamine transporter-2. *J. Neurochem.* **110,** 581–594
17. Vos, M. J., Hageman, J., Carra, S., and Kampinga, H. H. (2008) Structural and functional diversities between members of the human HSPB, HSPH, HSPA, and DNAJ chaperone families. *Biochemistry* **47,** 7001–7011
18. Cartier, E. A., Parra, L. A., Baust, T. B., Quiroz, M., Salazar, G., Faundez, V., Egaña, L., and Torres, G. E. (2010) A biochemical and functional protein complex involving dopamine synthesis and transport into synaptic vesicles. *J. Biol. Chem.* **285,** 1957–1966
19. Daugaard, M., Rohde, M., and Jäättelä, M. (2007) The heat shock protein 70 family: highly homologous proteins with overlapping and distinct functions. *FEBS Lett.* **581,** 3702–3710
20. Shaner, L., and Morano, K. A. (2007) All in the family: atypical Hsp70 chaperones are conserved modulators of Hsp70 activity. *Cell Stress Chaperones* **12,** 1–8
21. Géminard, C., Nault, F., Johnstone, R. M., and Vidal, M. (2001) Characteristics of the interaction between Hsc70 and the transferrin receptor in exosomes released during reticulocyte maturation. *J. Biol. Chem.* **276,** 9910–9916
22. Lu, H. A., Sun, T. X., Matsuzaki, T., Yi, X. H., Eswara, J., Bouley, R., McKee, M., and Brown D. (2007) Heat shock protein 70 interacts with aquaporin-2 and regulates its trafficking. *J. Biol. Chem.* **282,** 28721–28732
23. Hinzpeter, A., Lipecka, J., Brouillard, F., Baudoin-Legros, M., Dadlez, M., Edelman, A., and Fritsch J. (2006) Association between Hsp90 and the ClC-2 chloride channel upregulates channel function. *Am. J. Physiol. Cell Physiol.* **290,** C45-C56
24. Meimaridou, E., Gooljar, S. B., Ramnarace, N., Anthonypillai, L., Clark, A. J., and Chapple, J. P. (2011) The cytosolic chaperone Hsc70 promotes traffic to the cell surface of intracellular retained melanocortin-4 receptor mutants. *Mol. Endocrinol.* **25,** 1650–1660
25. Tobaben, S., Thakur, P., Fernández-Chacón, R., Südhof, T. C., Rettig, J., and Stahl, B. (2001) A trimeric protein complex functions as a synaptic chaperone machine. *Neuron* **31,** 987–999
26. Zinsmaier, K. E., and Bronk, P. (2001) Molecular chaperones and the regulation of neurotransmitter exocytosis. *Biochem. Pharmacol.* **62,** 1–11
27. Leshchyns'ka, I., Sytnyk, V., Richter, M., Andreyeva, A., Puchkov, D., and Schachner M. (2006) The adhesion molecule CHL1 regulates uncoating of clathrin-coated synaptic vesicles. *Neuron* **52,** 1011–1025
28. Machado, P., Rostaing, P., Guigonis, J. M., Renner, M., Dumoulin, A., Samson, M., Vannier, C., and Triller, A. (2011) Heat shock cognate protein 70 regulates gephyrin clustering. *J. Neurosci.* **31,** 3–14
29. Bowling, K. M., Huang, Z., Xu, D., Ferdousy, F., Funderburk, C. D., Karnik, N., Neckameyer, W., and O'Donnell, J. M. (2008) Direct binding of GTP cyclohydrolase and tyrosine hydroxylase: regulatory interactions between key enzymes in dopamine biosynthesis. *J. Biol. Chem.* **283,** 31449–31459
30. Swick, L., and Kapatos, G. (2006) A yeast 2-hybrid analysis of human GTP cyclohydrolase I protein interactions. *J. Neurochem.* **97,** 1447–1455
31. Wang, Z., Ferdousy, F., Lawal, H., Huang, Z., Daigle, J. G., Izevbaye, I., Doherty, O., Thomas, J., Stathakis, D. G., and O'Donnell, J. M. (2011) Catecholamines up integrates dopamine synthesis and synaptic trafficking. *J. Neurochem.* **119,** 1294–1305
32. Jin, H., Wu, H., Osterhaus, G., Wei, J., Davis, K., Sha, D., Floor, E., Hsu, C. C., Kopke, R. D., and Wu J. Y. (2003) Demonstration of functional coupling between γ-aminobutyric acid (GABA) synthesis and vesicular GABA transport into synaptic vesicles. *Proc. Natl. Acad. Sci. U.S.A.* **100,** 4293–4298
33. Hsu, C. C., Davis, K. M., Jin, H., Foos, T., Floor, E., Chen, W., Tyburski, J. B., Yang, C. Y., Schloss, J. V., and Wu, J. Y. (2000) Association of L-glutamic acid decarboxylase to the 70-kDa heat shock protein as a potential anchoring mechanism to synaptic vesicles. *J. Biol. Chem.* **275,** 20822–20828
34. Mosharov, E. V., Larsen, K. E., Kanter, E., Phillips, K. A., Wilson, K., Schmitz, Y., Krantz, D. E., Kobayashi, K., Edwards, R. H., and Sulzer, D. (2009) Interplay between cytosolic dopamine, calcium, and α-synuclein causes selective death of substantia nigra neurons. *Neuron* **62,** 218–229
35. Guo, J. T., Chen, A. Q., Kong, Q., Zhu, H., Ma, C. M., and Qin, C. (2008) Inhibition of vesicular monoamine transporter-2 activity in α-synuclein stably transfected SH-SY5Y cells. *Cell Mol. Neurobiol.* **28,** 35–47
36. Hastings, T. G., Lewis, D. A., and Zigmond, M. J. (1996) Role of oxidation in the neurotoxic effects of intrastriatal dopamine injections. *Proc. Natl. Acad. Sci. U.S.A.* **93,** 1956–1961
37. Hastings, T. G., Lewis, D. A., and Zigmond, M. J. (1996) Reactive dopamine metabolites and neurotoxicity: implications for Parkinson's disease. *Adv. Exp. Med. Biol.* **387,** 97–106
38. Sulzer, D., Bogulavsky, J., Larsen, K. E., Behr, G., Karatekin, E., Kleinman, M. H., Turro, N., Krantz, D., Edwards, R. H., Greene, L. A., and Zecca, L. (2000) Neuromelanin biosynthesis is driven by excess cytosolic catecholamines not accumulated by synaptic vesicles. *Proc. Natl. Acad. Sci. U.S.A.* **97,** 11869–11874
39. Chen, R., Wei, J., Fowler, S. C., and Wu, J. Y. (2003) Demonstration of functional coupling between dopamine synthesis and its packaging into synaptic vesicles. *J. Biomed. Sci.* **10,** 774–781
40. Caudle, W. M., Richardson, J. R., Wang, M. Z., Taylor, T. N., Guillot, T. S., McCormack, A. L., Colebrooke, R. E., Di Monte, D. A., Emson, P. C., and Miller, G. W. (2007) Reduced vesicular storage of dopamine causes progressive nigrostriatal neurodegeneration. *J. Neurosci.* **27,** 8138–8148
41. Chen, L., Ding, Y., Cagniard, B., Van Laar, A. D., Mortimer, A., Chi, W., Hastings, T. G., Kang, U. J., and Zhuang, X. (2008) Unregulated cytosolic dopamine causes neurodegeneration associated with oxidative stress in mice. *J. Neurosci.* **28,** 425–433

42. Lotharius, J., and Brundin, P. (2002) Pathogenesis of Parkinson's disease: dopamine, vesicles and α-synuclein. *Nat. Rev. Neurosci.* **3,** 932–942
43. Ding, Y. M., Jaumotte, J. D., Signore, A. P., and Zigmond, M. J. (2004) Effects of 6-hydroxydopamine on primary cultures of substantia nigra: specific damage to dopamine neurons and the impact of glial cell line-derived neurotrophic factor. *J. Neurochem.* **89,** 776–787
44. Ungewickell, E., Ungewickell, H., and Holstein, S. E. (1997) Functional interaction of the auxilin J domain with the nucleotide- and substrate-binding modules of Hsc70. *J. Biol. Chem.* **272,** 19594–19600
45. Funderburk, C. D., Bowling, K. M., Xu, D., Huang, Z., and O'Donnell, J. M. (2006) A typical N-terminal extensions confer novel regulatory properties on GTP cyclohydrolase isoforms in *Drosophila melanogaster*. *J. Biol. Chem.* **281,** 33302–33312
46. Morciano, M., Burré, J., Corvey, C., Karas, M., and Zimmermann, H., Volknandt W. (2005) Immunoisolation of two synaptic vesicle pools from synaptosomes: a proteomics analysis. *J. Neurochem.* **95,** 1732–1745
47. Egaña, L. A., Cuevas, R. A., Baust, T. B., Parra, L. A., Leak, R. K., Hochendoner, S., Peña, K., Quiroz, M., Hong, W. C., Dorostkar, M. M., Janz, R., Sitte, H. H., and Torres, G. E. (2009) Physical and functional interaction between the dopamine transporter and the synaptic vesicle protein synaptogyrin-3. *J. Neurosci.* **29,** 4592–4604
48. Parra, L. A., Baust, T., El Mestikawy, S., Quiroz, M., Hoffman, B., Haflett, J. M., Yao, J. K., and Torres, G. E. (2008) The orphan transporter Rxt1/NTT4 (SLC6A17) functions as a synaptic vesicle amino acid transporter selective for proline, glycine, leucine, and alanine. *Mol. Pharmacol.* **74,** 1521–1532
49. Perez, R. G., Waymire, J. C., Lin, E., Liu, J. J., Guo, F., and Zigmond, M. J. (2002) A role for α-synuclein in the regulation of dopamine biosynthesis. *J. Neurosci.* **22,** 3090–3099
50. Reinhard, J. F. Jr., Smith, G. K., and Nichol, C. A. (1986) A rapid and sensitive assay for tyrosine-3-monooxygenase based upon the release of $3H_2O$ and adsorption of [3H]-tyrosine by charcoal. *Life Sci.* **39,** 2185–2189